World Applied Sciences Journal 18 (7): 909-917, 2012
ISSN 1818-4952

DOI: 10.5829/idosi.wasj.2012.18.07.617

Numerical Simulation of Split Vane in a 60 Fuel Rod Bundle of VVER-440 Reactor and Survey the Effect of Large Length Split Vane (LLSV) and Half-Length Split Vane (HLSV) on Heat Transfer Distribution

[1]M.R. Abdi, [2]M. Asgari, [2]Kh. Rezaee Ebrahim Saraee and [3]M. Talebi

[1]Department of Physics, Faculty of Science, University of Isfahan, Isfahan 81746-73441, Iran
[2]Department of Nuclear Engineering, Faculty of Advanced Sciences and Technologies, University of Isfahan, Isfahan 81746-73441, Iran
[3]Nuclear Science and Technology Research Institute, Isfahan, Iran

Abstract: In the present study, the fuel bundle in the VVER-440 nuclear reactor is simulated and thermo-hydraulic parameters such as heat transfer coefficient; pressure drop and temperature of fuel rods are estimated. The most research that has been done is related to split vanes of square fuel bundle; however our objective in this study is to investigate split vanes of triangular fuel bundle. Due to lack of experimental results, the validity of CFD analysis of calculation is performed with three models of turbulence. The results showed that using split vane over the triangular fuel bundle led to decrease heat transfer coefficient while heat transfer coefficient is increased in square array fuel bundle.

Key words: CFD analysis · Fuel bundle · VVER-440

INTRODUCTION

Process analysis and design of nuclear reactors require both neutronics and thermo-hydraulic analysis. The study of transient thermo-mechanical phenomena in nuclear reactor fuel rods is of great importance because it is directly related to the problem of reactor safety [1, 2]. Most spacer grids are designed with mixing vanes which cause a cross and swirl flow between and within the sub-channels, enhancing the local heat transfer performance in the grid vicinity. The improvement of the heat transfer lead to higher operating power in the reactor [3]. It is necessary to know the transient temperature profile in the fuel rod. This research is concerned with the calculation of the transient temperature field only; mechanical and structural changes are not investigated here. The results of these analyses then will be used to design the primary and secondary loops.

The evaluation of the thermal-mixing performance is very important in the VVER fuel assembly design. The use of CFD code is very helpful in improving the design approval of the VVER fuel assembly, especially for the split vanes. From the view point of split vanes design, there are two main objects; one is the pressure drop and the other is the heat transfer coefficient.

In a nuclear power plant, an optimum heat removal from the surface of the nuclear fuel elements in a reactor is very important for the viewpoint of a reactor thermal margin and safety. Recently, due to the great advances in computation technology, commercial CFD codes are being used to design the optimized flow mixing device.

There have been many efforts to find the mechanism of a thermal mixing, pressure drop and shear stress in structure square sub-channel geometry [4-11]. Furthermore, there are some studies related to triangular fuel bundle in the literatures [12-14].

There is no study in the literature that is related to split vanes of triangular fuel bundle as result of our aim focused on investigating heat transfer coefficient, pressure drop and temperature parameters of fuel bundle in this array.

Modeling

CFD Modeling: VVER-440 is a pressurized water reactor with an open type of hexagonal core geometry that contains 349 fuel assemblies. The fuel assembly VVER-440 reactor consists of 127 fuel rods of diameter 9.1 mm arranged in hexagonal arrangements. The fuel rods long approximately 2.42 m with eleven spacer grids.

Corresponding Author: Mohammad Reza Abdi, Department of Physics, Faculty of Science, University of Isfahan, Isfahan 81746-73441, Iran. Tel: +98-9131026744.

For modeling a fuel assembly of VVER-440 first, 1/6 fuel assembly is considered and after solving fluid flow domain with governing equations this model generalized to the entire fuel assembly (Fig. 1).

Due to the limitations in computer hardware resources, it is difficult to analyze the whole of the flow field in the fuel bundle. Therefore, the 960 mm length of fuel bundle with four spacer grids and several fuel rods of the bottom of fuel assembly are selected for the analysis (Fig. 2).

In this study in total 61 fuel rod was simulated which center rod is without heat flux because is used as detector or source location. It is needed to mention that the simulated fuel assembly is in the center of fuel assembly of reactor. With modeling 1/6 fuel assembly, less computational time is needed also the model is closer to reality.

As shown in Fig. 2 the volume with length of 960 mm included 8 full diameter fuel rods and 4 fuel rods as half-full that located in symmetry boundary. Then spacer grid was simulated similar to those whom are used in VVER-440 (Fig. 3). The distance between spacer grids is 240 mm and height of those is 10 mm.

To using appropriate mesh density and mesh steady, first sample of model is defined as height 240 mm (Fig. 4), due to 240 mm of fuel assembly is repeated along the 960 mm (Fig. 5). Then after solving computational domain and find appropriate mesh density in this volume, this amount mesh density distribute to total model as height 960 mm with four spacer grids.

The resolution of mesh near the wall is shown in Fig. 6. Finally, split vanes on the spacer grids are simulated and t he effect of the split vanes on the thermo-hydraulic parameters is studied (Fig. 7). The simulation is considered with a specific plan therefore maximum swirling flow pattern will create in the sub-channel then this swirling flow is caused of preventing hot spots to occur on fuel rods (Fig. 8). The dimension of a split vane is shown in Fig. 9.

To investigating the effect of split vanes on thermo-hydraulics parameters three angles were defined ($\theta = 60°$, $\theta = 70°$ and $\theta = 80°$). Maximum performance of split vanes is in this range [15-17]. Again with considering split vanes and obtaining appropriate mesh density and mesh steady, sample of model is defined as height 240 mm with one spacer grid. After solving computational domain and find appropriate mesh density in this volume to effect thermo-hydraulic parameters, appropriate angle is selected ($\theta = 70°$). This amount mesh density distribute to total model as height 960 mm with four spacer grid.

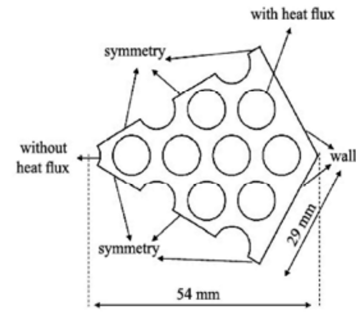

Fig. 1: Simulated 1/6 of fuel assembly of VVER-440

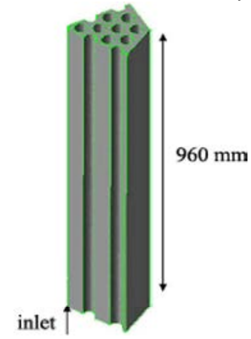

Fig. 2: The volume with length of 960 mm

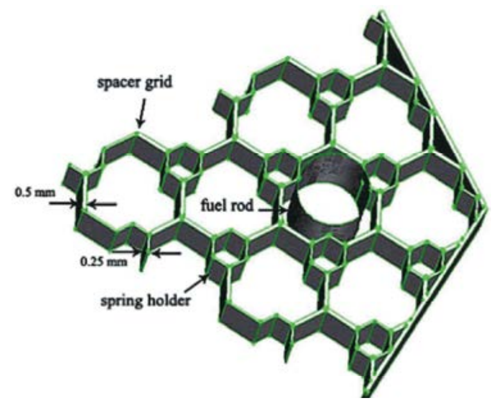

Fig. 3: The model of spacer grid

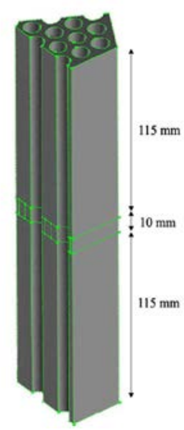

Fig. 4: The sample of model as height 240 mm for mesh steady

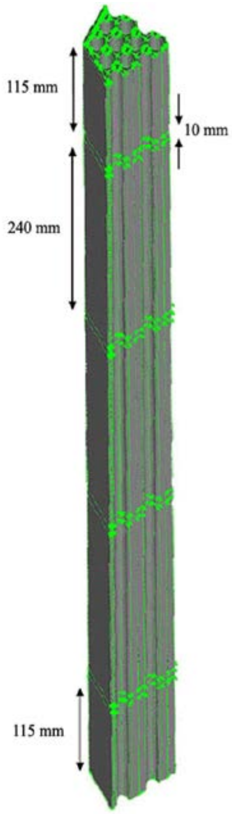

Fig. 5: The 960 mm length of fuel bundle with 4 spacer grids

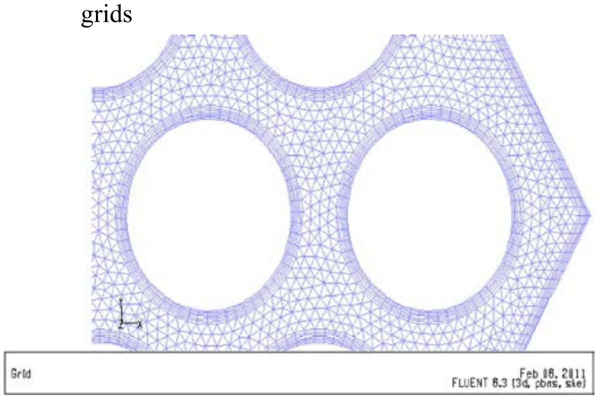

Fig. 6: The resolution of mesh near the wall

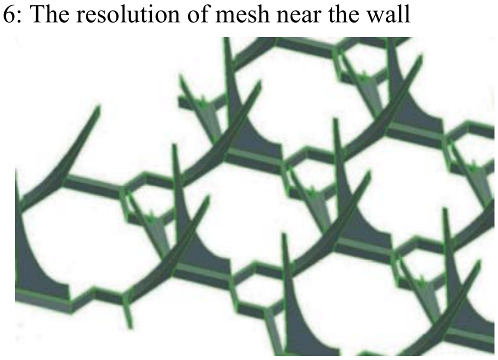

Fig. 7: The simulated split vanes on spacer grid

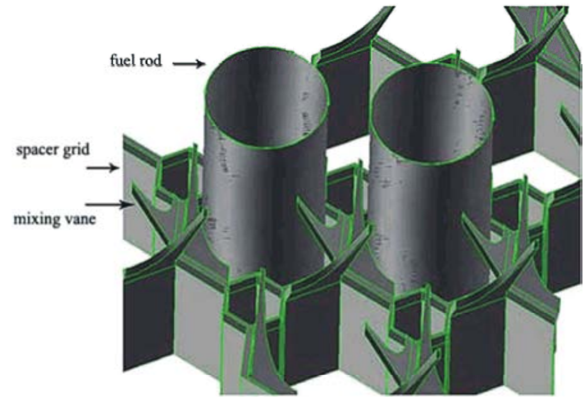

Fig. 8: View of split vanes between fuel rods

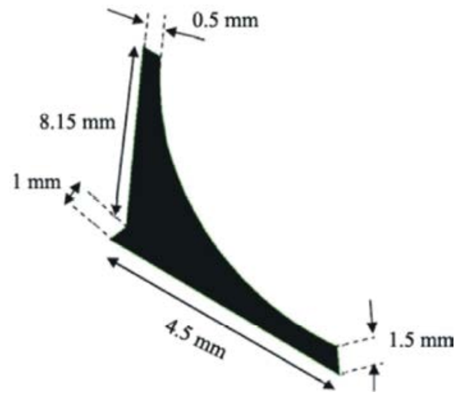

Fig. 9: The dimension of a split vane

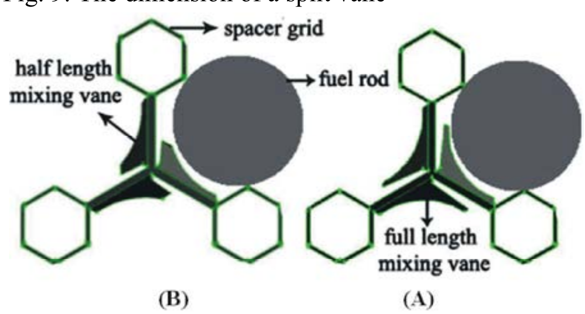

Fig. 10: (A): (LLSV), (B): (HLSV)

In order to compare effect of the length of split vanes on thermo-hydraulics parameters, the length of split vanes are reduced from 8.15 mm to half 4.075 mm. Plan view of CFD model for different geometries is shown in Fig. 10.

Boundary Condition: The inlet boundary conditions are used in these CFD simulations were taken from a model without the spacer. The working fluid is water at the respective experimental Conditions. The types of the boundary conditions were in accordance with the conditions of the 240 mm long model. At the lower end of the model inlet boundary condition was used. The inlet velocity of flow is 3.25 m/s and its temperature is 540 °K.

The turbulence boundary conditions are not known accurately, but according to Fluent Inc [18] turbulence intensity at inlet is concerned 3.5%. At the upper end of the bundle outlet condition of 0 Pa average static pressure was defined so that we can compute pressure loss. In these calculations the roughness of the walls was not taken into account and smooth walls were defined. Necessarily on the symmetry plans symmetry boundary conditions were used. In the core the thermal flux changes both in radial and axial directions, but in this study we defined heat flux as constant for all fuel rods.

The hydraulic diameter of the bundle is 7.782 mm. For the flow calculations, the solid surfaces of the fuel rod and spacer grid have no slip boundary condition and a symmetric condition was imposed on the other outer surface. In the thermal study, the heat flux over the fuel rods is specified. The heat flux, 1047.340 kW/m^2, specified over the surface of the rods, corresponds to the average value of the axial heat flux in modeling of the domain in the VVER-440 reactor at full power (1375 MW) but the maximal heat flux in the core is near to this. The Reynolds number for this inlet velocity is 1.932556×10^5 and is well inside the turbulent flow regime.

The well-known Fluent code was utilized to simulate the turbulence flow. At the wall surfaces of rod, grid spacers and split devices, no slip conditions were applied. The CFD analyses of this study used a standard under-relaxation factor for each of the governing equations and a special under-relaxation of the generalized periodic boundary conditions. The standard under-relaxation factor was set to a small value as low as 0.1. The calculation was terminated when the residuals for all governing equations were reduced to 10^{-5} and for energy equation 10^{-9} (Fig. 11).

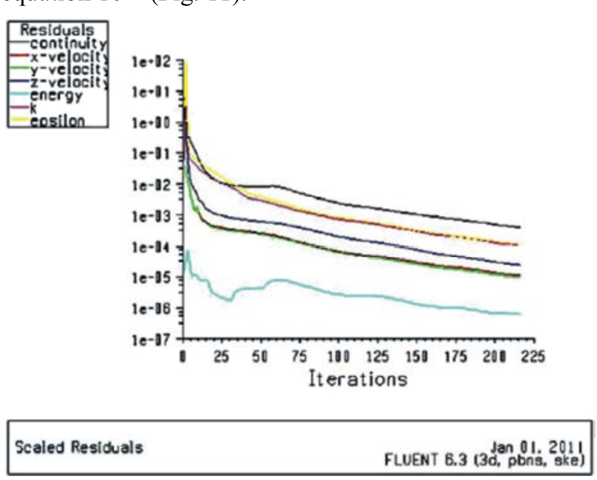

Fig. 11: Residuals for all governing equations to study convergence of the solution

Numerical Modeling: The equations that govern the fluid flow and heat transfer process in the rod bundle are continuity, momentum and energy. Furthermore, the standard k-ε model equations are as following:

$$\frac{\partial(\rho k)}{\partial t} + div(\rho k U) = div\left[\frac{\mu_t}{\sigma_k} grand\ k\right] + 2\mu_t E_{ij} - \rho E \tag{1a}$$

$$\frac{\partial(\rho \varepsilon)}{\partial t} + div(\rho \varepsilon U) = div\left[\frac{\mu_t}{\sigma_\sigma} grand\varepsilon\right] + C_{1\varepsilon}\frac{\varepsilon}{k} 2\mu_t E_{ij}, E_{ij} - C_{2\varepsilon}\rho\frac{\varepsilon^2}{k} \tag{1b}$$

and the k- ω – SST model equations are:

$$\frac{\partial}{\partial t}(\rho\kappa) + \frac{\partial}{\partial x_i}(\rho\kappa u_i) = \frac{\partial}{\partial x_j}\left(\Gamma_\kappa \frac{\partial x}{\partial x_j}\right) + \breve{G}_\kappa - Y_\kappa + S_\kappa \tag{2a}$$

$$\frac{\partial}{\partial t}(\rho\omega) + \frac{\partial}{\partial x_i}(\rho\omega u_i) = \frac{\partial}{\partial x_j}\left(\Gamma_\omega \frac{\partial \omega}{\partial x_j}\right) + \breve{G}_\omega - Y_\omega + S_\omega + D_\omega \tag{2b}$$

and the spalart-allmaras model equation:

$$\frac{\partial z}{\partial t} + u_i\frac{\partial z}{\partial x_i} = \frac{\partial}{\partial x_i}\left(\frac{\sqrt{kl}}{\sigma_z}\frac{\partial z}{\partial x_i}\right) + c_{zl}\frac{z}{k}P_k - c_{2z}z\frac{\sqrt{k}}{l} + S \tag{3}$$

where $\delta_z, c_{zi}.c_{2z}$ and P_k are empirical constants.

The finite volume method with the k-ε turbulence model is employed in the analysis.

RESULTS AND DISCUSSION

The mesh sensitivity study is done for fuel rod without spacer grid for three different amounts of mesh (3100000, 4050000 and 5000000 mesh). We have defined the linear coordinates A: (x= 0.0305, y = 0.0035, z = 0.015-0.975) and surveyed our results along this line in sub-channel (Fig. 12, 13).

According to Figures 12 and 13 can be seen that 4050000 mesh more appropriate than two others. Fig. 12 shows that velocity profile start from 3.25 m/s to 3.67 m/s and then is reached to developed state and quickly going to steady state. Because of growth boundary layer the velocity is increased along the channel which is due to viscous effects on the flow, although the output average velocity equals the speed of the input equals to 3.25 m/s.

To survey the effect of spacer grids, the sample model is used as height 240 mm for 3 amount of meshes (700000, 1850000 and 3000000) along line B: (x = 0.02895, y = 0, z = 0.015-0.975) that according to Figure 14a and 14b, by comparing, 1850000 is chosen due to meshes 1850000 and 3000000 have more overlap than other one.

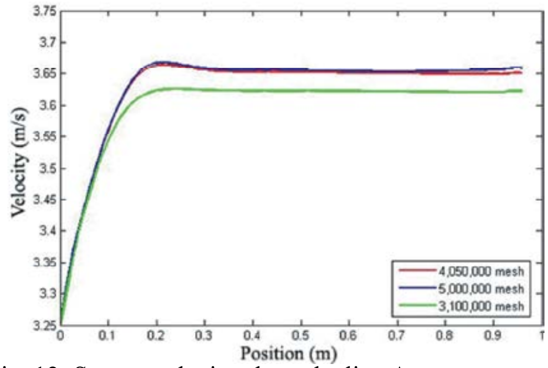

Fig. 12: Survey velocity along the line A

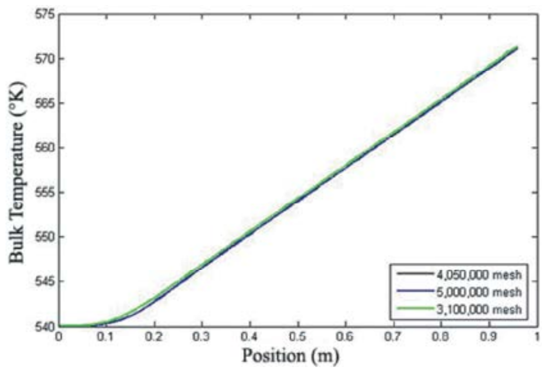

Fig. 13: Survey bulk temperature along the line A

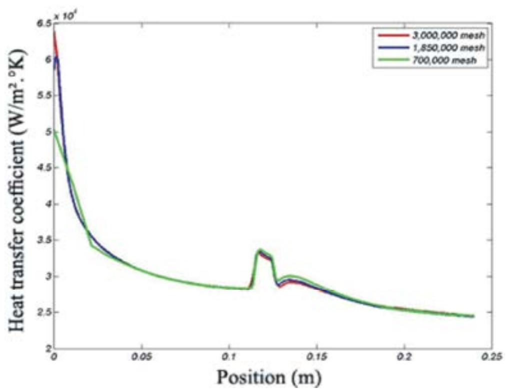

A

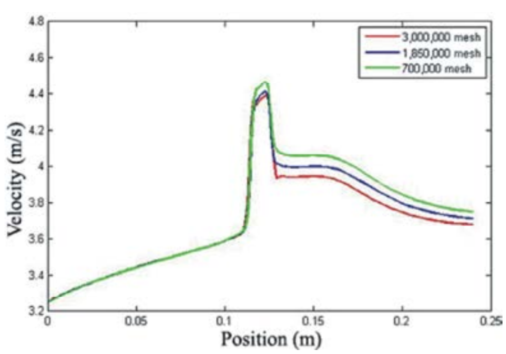

B

Fig. 14: (A) Study heat transfer coefficient along the line B, (B). Study velocity along the line B

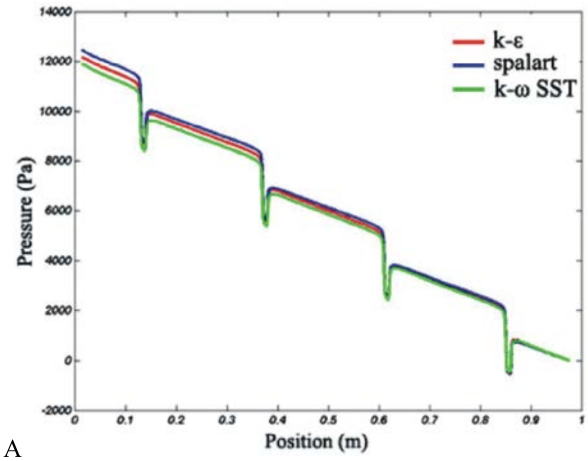

A

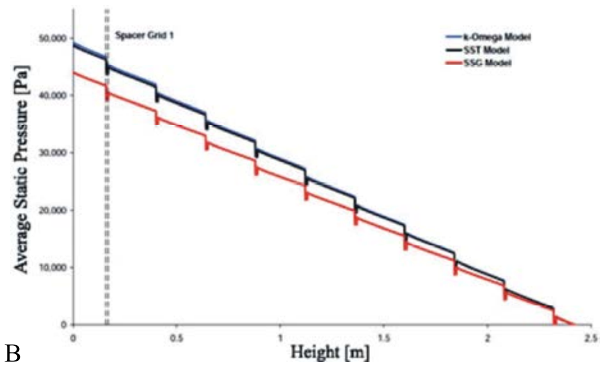

B

Fig. 15: (A) The average pressure drop in the flow direction, (B). The analysis of average pressure drop in the flow direction computed by Tóth in 2006 [22]

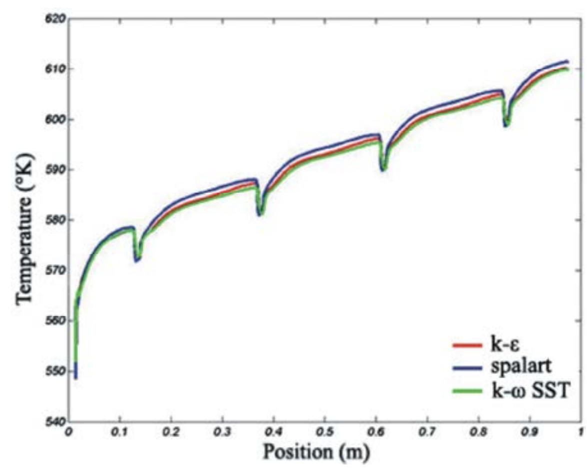

Fig. 16: The average temperature of clad in the flow direction

In the next step we used this density of mesh in total fuel bundle with 4 spacer grids. Due to the lack of experimental results three different turbulence models were used. Our results were compared to analysis that published by Tóth and Aszódi in 2006 [1, 19]. The average pressure distribution is shown in Fig. 15 which contains the three parts of the pressure drop [11]. The pressure drop is created due to the spacer grids, gravity and the friction on the fuel rods and on the shroud.

The effect of the four spacer grids on the static pressure is quite clear in Fig. 15(a).

Because of the cross section of sub-channel in spacer grids is smaller than its sub-channel; the flow velocity is increased in the spacer grids as result of pressure drop is increased. Behind the spacer grids the velocity rapidly is decreased and then the static pressure is increased until to achieve a value which is less than in front of the spacer grids. The pressure drop for each spacer grid is equal to 815 Pa. Tóth in 2006 computed this amount approximately 1570 Pa, although his simulated model included 24 rods but model that is simulated in this investigation includes 12 rods [19]. In other to if his model would contains 12 rods, the pressure drop for each spacer grid was 785 Pa (Fig. 15(b)).

In Fig. 16, it can be seen that the cladding average temperature is decreased at the spacer grids. When the coolant flows into the holes of the spacer grids rapidly, the velocity and the turbulence kinetic energy is grown therefore the conditions of heat transfer is improved. (See heat transfer coefficient in Fig. 17) and in diagram of temperature-length of fuel bundle, there is a temperature drop in location of spacer grid.

Behind the spacer grid, the temperature of the cladding is decreased, because the velocity is increased (Fig. 18). Therefore, the conditions of the heat transfer are well and the heat transfer coefficient is increased. This process alternatively occurs in all spacer grids.

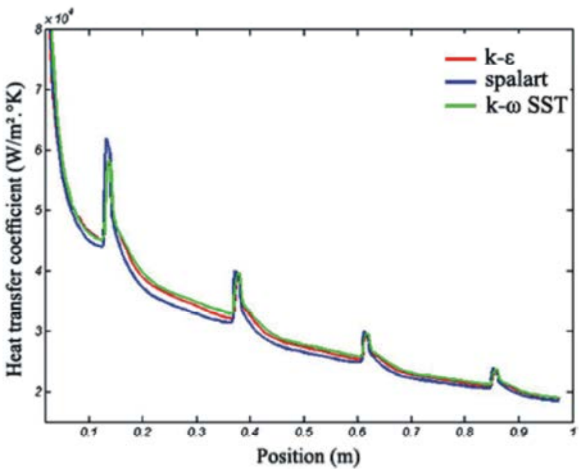

Fig. 17: The average heat transfer coefficient in direction of the clad

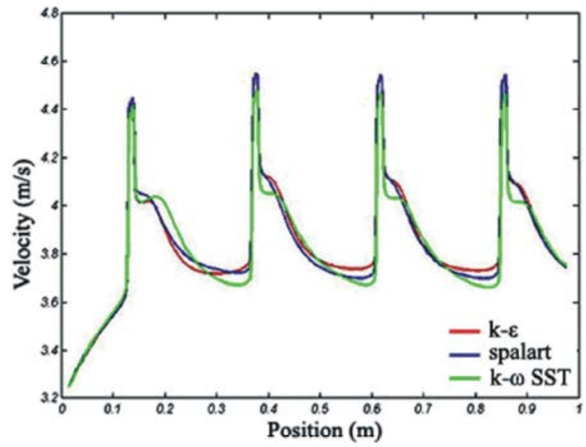

Fig. 18: The average velocity in the flow direction

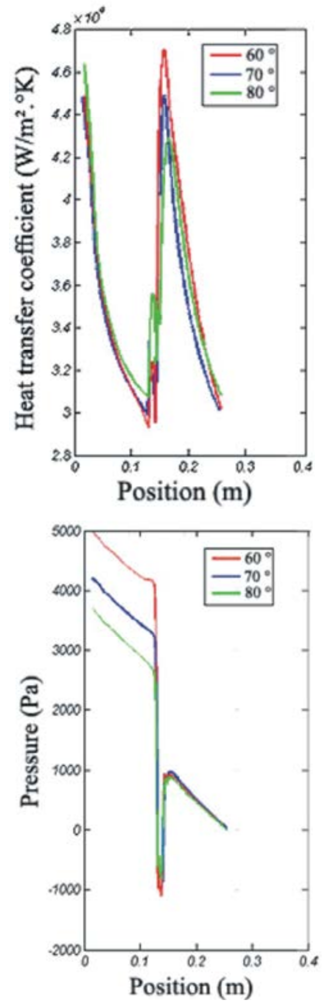

A

B

Fig. 19: (A) Study average heat transfer coefficient of the clad to select the optimum angle, (B). Study average pressure in the flow direction to select the optimum angle

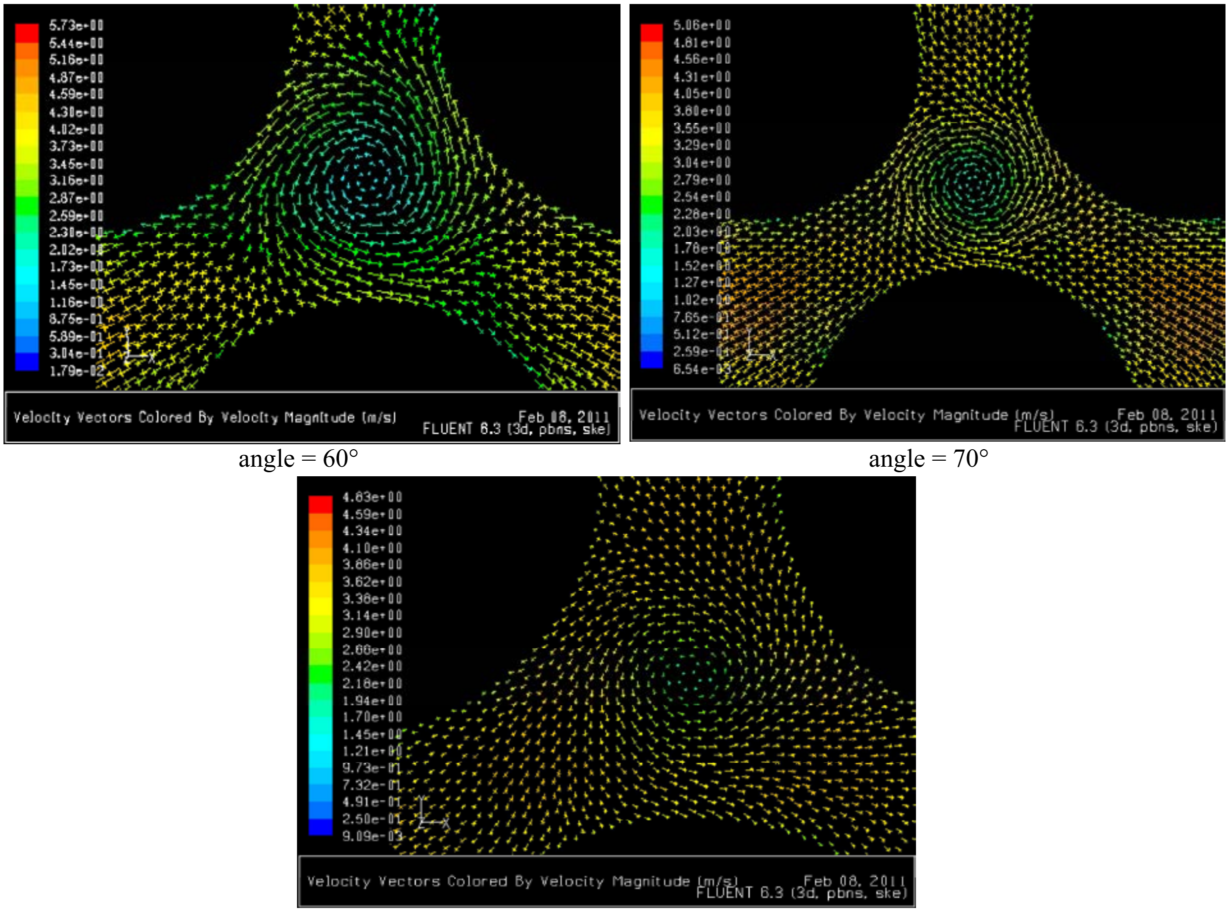

angle = 60° angle = 70°

angle = 80°

Fig. 20: Swirling vector of flow is created by three angles

For rod bundles constructed using a series of spacer grids, the axial spacing between the spacer grids can be long enough for fully-developed flow conditions to develop in the span between two consecutive spacer grids. This also indicates that the flow has reached full development at 34 hydraulic diameters and 14 hydraulic diameters after spacer grid.

The secondary flow intensity is defined as the magnitude of the secondary flow vector divided by axial bulk mean velocity. Even if its magnitude is small, is important because it greatly influences the promotion of heat transfer from rods to sub channels and affects the mean axial velocity, turbulent kinetic energy and wall shear stress distributions.

Split Vanes: The effect of split vanes on thermo hydraulic parameters is surveyed in three angles (60°, 70° and 80°) because of in this range; the effect of split vanes is max.

It is clear from Fig. 19 (a) and 19 (b), not the pressure drop of split vanes with angel of 70° but heat transfer coefficient is more than others. Moreover, according to the Fig. 20, maximum swirling vector of flow is created in angel 70° as a result of this angel is used for split vanes on all spacer grids.

At next step pressure drop and heat transfer coefficient with angel of 70° and the vanes with half-length is compared (Fig. 21 and 22). Heat transfer coefficient of full length split vanes is larger than half length split vanes. This is because of blocking higher area of flow sub-channel then is created more back flows. In this case, the part of the rods behind the split vanes due to neighbor with higher temperature fluid in the more time, the cooling is less and heat transfer is reduced. However, due to more turbulence in the half- length split vanes, heat transfer coefficient is larger than full length split vanes. Also pressure drop is higher than half-length split vanes.

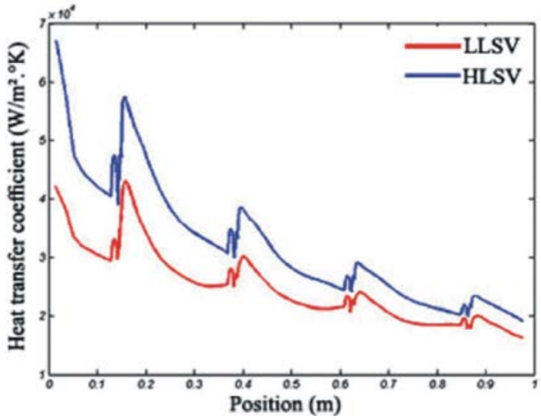

Fig. 21: Comparison of average heat transfer coefficient of (LLSV) and (HLSV)

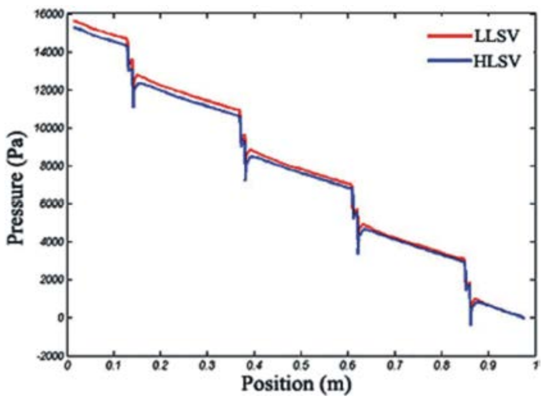

Fig. 22: Comparison of average pressure drop of (LLSV) and (HLSV)

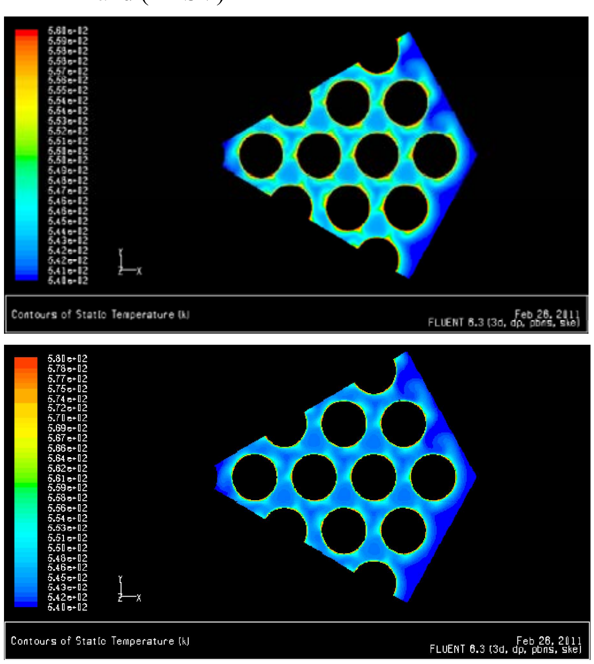

Fig. 23: The temperature distribution in A: (LLSV) and B: (HLSV)

The temperature distribution in half-length split vanes is better compared to full length (Fig. 23). The better temperature distribution has positive effect on heat transfer between cooling fluids and clad of the fuel rods.

CONCLUSIONS

In the present study, the fuel bundle in the VVER-440 nuclear reactor is simulated and thermo hydraulic parameters such as heat transfer coefficient, pressure drop and temperature of fuel rods are estimated. Then by simulating four spacer grids, the effects of these spacer grids on thermo hydraulic parameters are investigated. Finally, split vanes on the spacer grids are simulated and the effect of the split vanes on the thermo hydraulic parameters is studied. The k-ε and energy equations with the k-ω and spallart-Almaras models for the turbulent are solved to determine the effect of spacer grids alone and spacer grids with split vanes which these split vanes reduce the axial velocity and increase the radial velocity.

The results showed that using spacer grids over the fuel bundle led to increased heat transfer coefficients. However, these grids increase pressure drop. For the split vanes a lower heat transfer coefficient is observed which is due to blocking the channel cross sections and induced back flow which also cause significant increase in pressure drop. The increased heat transfer coefficient in percent for spacer grids, full length split vanes and half-length split vanes are 49.55, 9.62 and 24.67, respectively. This explains why the split vanes are not used in the VVER reactors.

REFERENCES

1. Aszódi, A. and S. Tóth, 2008. CFD analysis of flow field in a triangular rod bundle, Nuclear Engineering and Design, 21(8): 352-363.
2. Almenas, K. and R. Lee, 1943. Introduction to Physical Nuclear Engineering, 2nd Edition, The American Nuclear Society.
3. Navarro, M. and A. Santos, 2011. Evaluation of numeric procedure for flow simulation of a 5×5 PWR rod bundle with a mixing vane spacer, Progress in Nuclear Energy, pp: 1-7.
4. Rehme, K., 1973. Pressure drop correlations for fuel element spacers, Nuclear Technology, 17: 15-23.
5. Rehme, K. and G. Trippe, 1980. Pressure drop and velocity distribution in rod bundles with spacer grids, Nuclear Engineering and Design., 62: 349-359.

6. Caraghiaur, D., W. Frid and N. Tillmark, 2004. Detailed pressure drop measurements in single- and two-phase adiabatic air-water turbulent flows in realistic BWR fuel assembly geometry with spacer grids. In: The 6th International Conference on Nuclear Thermal Hydraulics, Operations and Safety (NUTHOS-6), Nara, Japan, October 4-8 (paper ID N6P207).
7. Yang, S.K. and M.K. Chung, 1998. Turbulent flow through spacer grids in rod bundles, Journal of Fluids Engineering, 120: 786-791.
8. Chang, D. and S. Tavoularis, 2005. Unsteady numerical simulations of turbulence and coherent structures in axial flow near a narrow gap, Trans. ASME, 127: 458-466.
9. Chang, D. and S. Tavoularis, 2006. Convective heat transfer in turbulent flow near a gap, J. Heat Transfer, 128: 701-708.
10. Tzanos, C., 2004. Computational fluid dynamics for the analysis of light water reactor flows, Nuclear Technology, 147: 181-190.
15. Lee, C.M. and Y.D. Choi, 2007. Comparison of thermal-hydraulic performances of large scale vortex flow (LSVF) and small scale vortex flow (SSVF) mixing vanes in 17×17 nuclear rod bundle. Nuclear Engineering and Design., 237: 2322-2331.
16. Kjellström, B., 1972. Studies of Turbulent Flow Parallel to a Rod Bundle of Triangular Array. AB Atomenergie, Studsvik, Sweden, AE-RL-1344.
17. Trupp, A.C. and R.S. Azad, 1975. The structure of turbulent flow in triangular array rod bundles. Nucl. Eng. Des., 32: 47-84.
18. Böttcher, M., 2008. Primary loop study of a VVER-1000 reactor with special focus on coolant mixing, Nuclear Engineering and Design., 240: 2244-2253.
19. Dong, Z. and Y. Shen, 1991. An investigation of cross flow mixing effect caused by grid spacer with mixing blades in a rod bundle. Nuclear Engineering and Design, 125: 111-119.
20. Wang Kee, I., O. Dong and T. Hyun Chun, 2001. Flow analysis for optimum design of mixing vane in a PWR fuel assembly. Journal of the Korean Nuclear Society, 33: 327-338.
20. Byung Soo, S. and C. Soon, 2009. CHF experiment and CFD analysis in a 2×3 rod bundle with mixing vane. Nuclear Engineering and Design, 239: 899-912.
21. FLUENT Inc., 2001. Fluent 6.0 User's Guide.
22. Tóth, S. and A. Aszódi, 2006. Calculations of coolant flow in a VVER-440 fuel bundle with the code ANSYS CFX 10.0. In: Proceedings of the Workshop on Modeling and Measurements of Two-Phase Flows and Heat Transfer in Nuclear Fuel Assemblies, Stockholm, Sweden.